On the Nature of the Poloidal Component of the Sun's Magnetosphere

Dmitry G. Kiryan, George V. Kiryan

Institute of Problems of Mechanical Engineering of RAS
61 Bolshoy Prospect V.O., 199178, Saint-Petersburg, Russia
e-mail: diki.ipme@gmail.com

In this work we have found out such a sequence of physical processes which allowed us to reveal the cause-and-effect relationship between the observed poloidal alternating magnetic field of the Sun and a factor of a non-electromagnetic nature, which is external to the Sun. Specific character of the Sun's orbital motion about the Solar system barycenter promotes emergence inside the Sun of the conditions necessary for generation of the observed poloidal component of the Sun's magnetosphere without participation of the Sun's own rotation. Using a pendulum as a model, we have shown in what way the external impact upon the Sun initiates within the Sun itself forced oscillations which are just those that induce the poloidal alternating magnetic field; in its turn, this magnetic field defines the cyclic character of the Wolf numbers.

We have also revealed a process which allowed putting into consideration a natural event-time scale that may be quite useful in planning the observations and also in systematizing and synchronizing fragments of the available time series of observations manifesting the Sun's poloidal magnetic field about 20 years in period.

Keywords: Sun's poloidal magnetic field, inversion, pole flip, barycenter, Jupiter, Saturn, Wolf numbers

If you desire to return to the truth you
do not need to search for the road.
You know it. You have come down that way.
Retrace your footsteps.

Bernardus Claraevallensis

1 Problem definition

In studying sunspot radiation spectra, *George E. Hale* revealed in 1908 manifestations of the Zeeman effect[1], thus being the first who established the presence of the sunspot magnetic field; in 1953, American astronomers *Harold Delos Babcock* & *Horace Welcome Babcock* found out weak poloidal magnetic field of the Sun [2, 3, 4].

Since that time and up today, the scientific community continues systematically studying various aspects of the Sun's magnetosphere including the poloidal alternating magnetic field. There is still no clear common concept of this field generation mechanism, that is, what underlies this phenomenon, either factors external to the Sun or internal processes in the Sun itself.

Research object.

Poloidal alternating magnetic field of the Sun.

Let us consider Fig. 1 that demonstrates orientation of magnetic-field vectors $\underline{B}_{\mathbb{N}}$ and $\underline{B}_{\mathbb{S}}$ at the Sun's geographic poles, north pole $\mathbb{N}$ and south pole $\mathbb{S}$. These vectors are co-directional and lie on the axis of the Sun's own rotation (dashed line) which passes through point A, that is, the Sun's center of mass. The right part of the figure shows the dynamics of the Sun's magnetosphere poloidal component which is expressed through variations in the poloidal magnetic field strengths $B_{\mathbb{N}}$ and $B_{\mathbb{S}}$ at the Sun's north and south pole, respectively.

$$\underline{B}_{\mathbb{N}} \uparrow\uparrow \underline{B}_{\mathbb{S}} , \qquad B_{\mathbb{N}} = \underline{B}_{\mathbb{N}} \cdot \underline{n}_{\mathbb{N}} , \quad B_{\mathbb{S}} = \underline{B}_{\mathbb{S}} \cdot \underline{n}_{\mathbb{S}} , \tag{1}$$

where $\underline{n}_{\mathbb{N}}$, $\underline{n}_{\mathbb{S}}$ are the local normals at the poles in the northern and southern hemispheres of the Sun. Observations show that the poloidal component of the Sun's magnetosphere occurs approximately every 20 years. A sequence

[1] In 1896, Dutch researcher *Pieter Zeeman* revealed in studying the influence of external magnetic field on a radiation source the effect of spectral lines splitting [1].

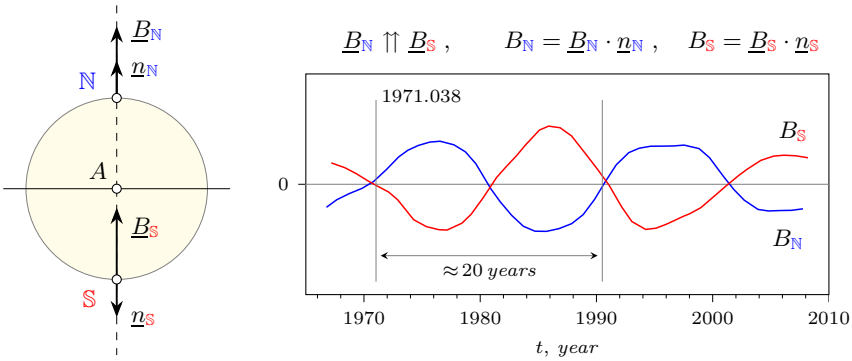

Figure 1. Variations in the Sun's magnetosphere. Fragments of time series $B_{\mathbb{N}}$ and $B_{\mathbb{S}}$ taken from [5], which reflect variations in the poloidal magnetic field at the respective geographic poles of the Sun.

of key moments reflecting the evolution of magnetic field strength $B_{\mathbb{N}}$ at the north pole of the Sun may be presented as follows:

$$\ldots \to B_{\mathbb{N}}{>}0 \to \overbrace{\mathbf{0} \to B_{\mathbb{N}}{<}0 \to \mathbf{0}}^{\approx 10 \text{ year}} \to B_{\mathbb{N}}{>}0 \to \overbrace{\mathbf{0} \to B_{\mathbb{N}}{<}0 \to \mathbf{0}}^{\approx 10 \text{ year}} \to \ldots \qquad (2)$$

≈ 20 year

The sequence of events at the south geographic pole of the Sun may be presented in the similar way.

The objective of the study.

> *The goal of this work is to reveal a sequence of cause-and-effect relationships between non-electromagnetic factors external to the Sun and the observed Sun's poloidal alternating magnetic field.*

As in problems with a "long-term" history and ambiguous results, we believe right to return to the time moment when it became evident that the Sun's poloidal magnetic field changes its polarity regularly.

2 The Sun and its orbit

The central object of our Solar System, which merely provides its physical existence, is the Sun whose mass is 99.86% of the total Solar System mass. Let us consider some key characteristics of the Sun in view of mechanics.

The Sun's internal structure is presented in Fig. 2. The Sun rotates counterclockwise with angular velocity $\omega_{\odot}$ about the axis passing through the

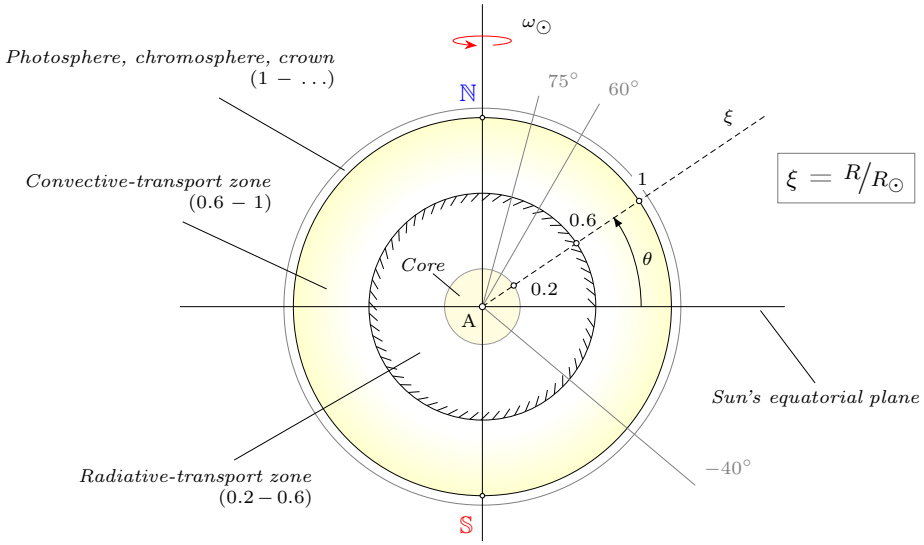

Figure 2. The Sun's internal structure (schematic diagram).

Sun's center of mass A and *geographic* poles ℕ and 𝕊. Doppler observations of the solar surface fix a differential rotation with the period of 25 days in the equatorial region and of up to 35 days at high latitudes. Let us put into consideration a dimensionless radial coordinate ξ, that is, a ratio between radial distance R of the considered point inside the Sun and Sun's average radius $R_\odot$. As the main regions of the Sun's internal structure, we regard the core, zones of the radiative and convective transport, and photosphere. The core is a spherical region with radius $\xi = 0.2$. The region immediately surrounding the solar core is referred to as the radiative-transport zone; it spreads as far as to $\xi = 0.6$. In its turn, the radiative-transport zone is surrounded by the convective-transport zone; the next region is the photosphere, and so on. In Fig. 2, the hatching indicates the spherical layer that is the contact boundary between the zones of radiative and convective transport. Such a concept of the Sun's internal structure is based on the helioseismology data [6, 7] which allowed the researchers to calculate the radial distribution of the intrasolar matter rotation frequency at different latitudes (Fig. 3, left panel). Analysis of this group of curves showed that there exists a specific solar region $\xi = 0.6$ in radius, which rotates with almost constant rate $\mathrm{f}(\xi, \theta) \approx 440\ nHz$. This region comprises the core and radiative-transport zone. Beyond this region one can see a sharp change in the rotation rate followed by its turning to non-linear behavior. The curves in the Fig. 3 right panel present the results of recalculating the Sun's rotation rate $\mathrm{f}(\xi, \theta)$ into linear rotation speed $v^*(\xi, \theta)$. Points ξ_{45}, ξ_{60}, ξ_{75} indicate the rotation radius at which speed v^* begins deviating from the linear dependence characteristic

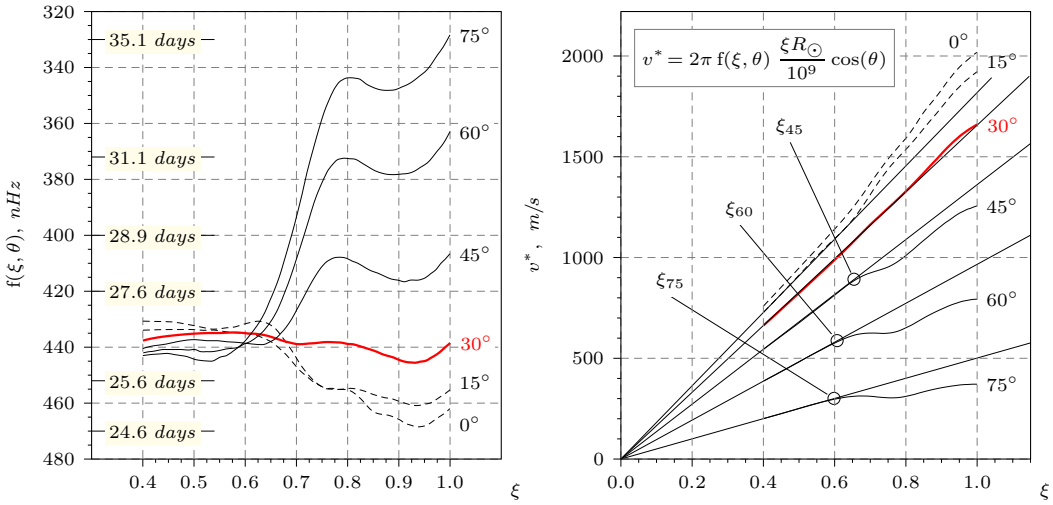

Figure 3. Distribution of the Sun's rotation rate $\mathrm{f}(\xi,\theta)$ and relevant linear speed v^* along radius ξ at latitudes $\theta=\{0°, 15°, 30°, 45°, 60°, 75°\}$.

of a rotating rigid (non-deformable) body.

Thus, analysis of the rotation-rate curves presented in Fig. 3 allows affirming that the Sun's central part (the core and radiative-transport zone) $\xi=0.6$ in radius rotates as a rigid body. All which surrounds the central part of the Sun, that is, the convective-transport zone, photosphere, *etc.*, exhibits, to various extents, the properties similar to those of a viscous liquid or gas.

Solar density. The radial distribution of density and mass are presented in Fig. 4. Notice that the core and radiative-transport zone together are

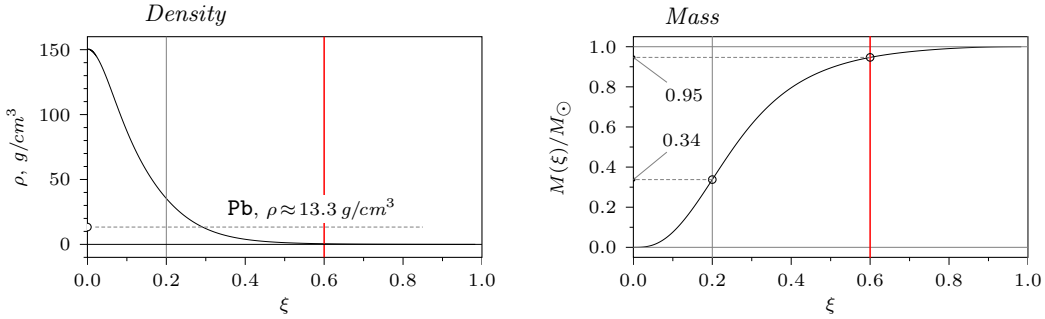

Figure 4. Radial distribution of solar density $\rho(\xi)$ and mass $M(\xi)$.

about 95% of the total mass of the Sun. The solar mass is also characterized by the gravitational field strength on the Sun's surface which is about $274\ m/s^2$, namely, 28 times higher than that of the Earth.

Sun's orbital motion. Fig. 5 demonstrates a fragment of orbital motion of the Sun's center of mass (point A) in the barycentric frame of reference. Analysis of the Sun's ephemeris[2] shows that the sidereal period of the Sun's

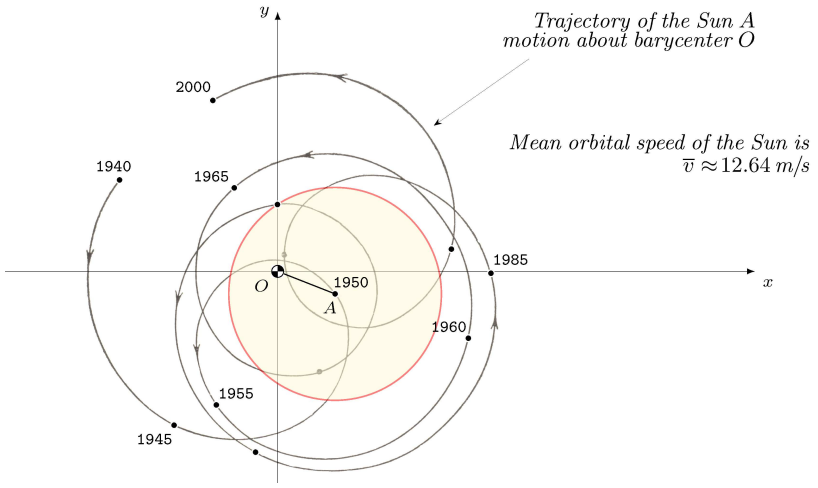

Figure 5. A fragment of projection of the trajectory of the Sun's center of mass A on ecliptic plane Oxy (from the book by P.G. Kulikovsky [8]).

own rotation about the barycenter is about 11.86 years.

Notice also that the Sun's orbital speed is not constant; it varies from $8.5\ m/s$ to $16.1\ m/s$, the mean value is $\overline{v} \approx 12.64\ m/s$. The radius of the Sun's orbit changes respectively according to the principle of conservation of momentum (principle of momentum conservation). The maximal distance between the Sun and Solar System barycenter does not exceed 2 solar radii. The solar equator inclination to the ecliptic is $\approx 7°15'$. More data on the Sun may be found in many papers, for instance, in the fundamental study [9].

3 The external factor and poloidal alternating magnetic field of the Sun

In the framework of the heuristic approach to the object of research (p. 3), let us present on one and the same time scale (Fig. 6) two physically different processes associated with the Sun, namely, variation in the Sun's orbital speed Δv and time series reflecting the poloidal magnetic field strengths $B_{\mathbb{N}}$, $B_{\mathbb{S}}$ at the Sun's north and south poles, respectively. To construct those

[2]Ephemerides are the tables containing calculated coordinates of the Sun, planets, stars and other celestial bodies in a relevant frame of reference for preset time moments.

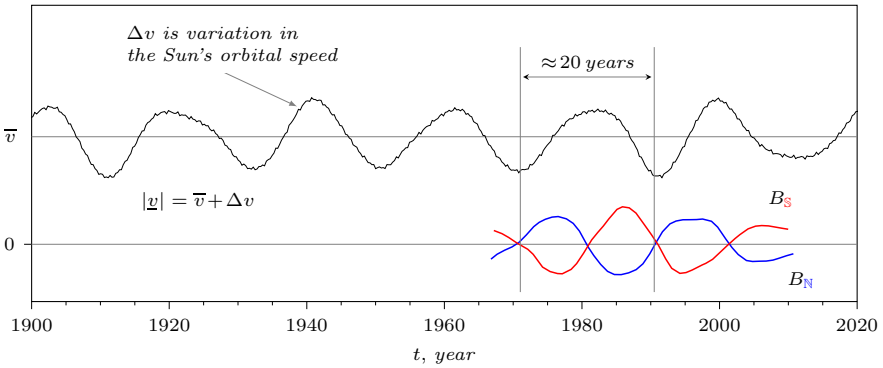

Figure 6. Comparison of the Sun's orbital speed variation Δv with oscillations in poloidal magnetic field strengths $B_{\mathbb{N}}$, $B_{\mathbb{S}}$ at respective solar poles.

curves, observation data given in the following publicly available sources were used:

- *NASA JPL Horizons* [10] — ephemerides of the Sun and planets.
- *WSO Polar Field Observations* [11] — poloidal magnetic field strengths at the solar poles.

Fig. 6 demonstrates a high extent of temporal consistency of the variation in the Sun's orbital speed Δv with the magnetic field oscillations at the solar poles. The poloidal configuration of the Sun's magnetosphere repeats every 20 years. This process is accompanied by the field inversion (pole flip); this means that the poloidal magnetic field strengths at the solar poles become zero simultaneously, i.e., $B_{\mathbb{N}} = B_{\mathbb{S}} = 0$. The inversion occurs every time the Sun's orbital speed $|\underline{v}|$ reaches its local extremum (minimum or maximum). When the Sun's orbital acceleration $|\dot{\underline{v}}|$ reaches its extremum, the solar poles exhibit the maximal poloidal magnetic field strengths. The obvious relationship between the processes illustrated in Fig. 6 allowed us to surely assume that

> *oscillations of the Sun's poloidal magnetic field are governed only by the 20-year variation Δv in the speed of the Sun's orbital motion about the Solar System barycenter.*

Indeed, in the framework of classical mechanics we can hardly assume the opposite, namely, that intrasolar processes are able to affect the non-uniformity of orbital motion of the Sun itself about the Solar System barycenter (Fig. 5).

However, that's the question: what is that external factor initiating the well-pronounced 20-year variation in the Sun's orbital speed? The Solar System is a closed system of gravitating bodies staying in dynamic equilibrium.

Indeed, the Sun's orbital speed variation Δv about 20 years in period is undoubtedly a result of gravitational interaction between all the Solar System material bodies except for dark matter [12, 13]. Again, based on heuristics, let us restrict the number of the Solar System gravitating bodies to only those that can significantly affect the Sun's orbital speed. Let them be Jupiter (J) with the period of ≈ 11.86 years and Saturn (S) with the period of $\approx$29.45 years. Notice that the solar mass is $\approx$99.86% of the Solar System mass, while the share of Jupiter and Saturn in the remaining 0.14% is about 88%.

Let us consider characteristic aspects of the mutual spatial arrangement of the chosen planets and Sun by using their ephemerides [10]. Fig. 7 demonstrates the relationship of the spatial-temporal configuration of the Sun, Jupiter and Saturn with the observed magnetic field strengths $B_{\mathbb{N}}$ and $B_{\mathbb{S}}$ at the respective solar poles. The Jupiter and Saturn mutual arrangement is characterized by function $L(t)$ that is the inverse squared distance between those planets and also by angular distance $\Delta\lambda$ between them. Time moments t_A, t_C, t_E fix the occurrence of the magnetic field inversion (pole flip), while t_B, t_D, t_F correspond to the maximal strengths of the poloidal magnetic field at the solar poles. Mutual arrangement of the Sun, Jupiter and Saturn is shown for each of these key time moments in the barycentric frame of reference. The red line indicates the instantaneous direction of the centrifugal force applied to the Sun's center of mass A.

Table 1 presents the key time moments for the *Sun-Jupiter-Saturn* system with indicating the *Jupiter-to-Saturn* angular distance $\Delta\lambda$ and the state of the Sun's magnetosphere. Superscripts $(+)$ and $(-)$ at $B_{\mathbb{N}}$, $B_{\mathbb{S}}$ indicate whether the relevant extremum is positive or negative. Thus, analysis of

Table 1. Time moments fixing the specific state of the Sun's magnetosphere. $\Delta\lambda$ is the angular distance between the Jupiter and Saturn; JD, GD are Julian and Gregorian dates, respectively.

—	JD	GD	$B_{\mathbb{N}}, B_{\mathbb{S}}$	$L(t)$	$\Delta\lambda$, *degree*	
t_A	JD 2440966.5	19710115	0	*min*	178.8	(180)
t_B	JD 2442816.5	19760208	$B_{\mathbb{N}}{}^{+}, B_{\mathbb{S}}{}^{-}$		89.9	(90)
t_C	JD 2444706.5	19810412	0	*max*	1.1	(0)
t_D	JD 2446546.5	19860426	$B_{\mathbb{N}}{}^{-}, B_{\mathbb{S}}{}^{+}$		90.1	(90)
t_E	JD 2448076.5	19900704	0	*min*	179.6	(180)
t_F	JD 2450026.5	19951105	$B_{\mathbb{N}}{}^{+}, B_{\mathbb{S}}{}^{-}$		90.2	(90)
t_G	JD 2451716.5	20000621	0	*max*	1.2	(0)
t_H	JD 2453796.5	20060302	$B_{\mathbb{N}}{}^{-}, B_{\mathbb{S}}{}^{+}$		90.1	(90)

the mutual arrangement of the Sun, Jupiter and Saturn shows that inversion

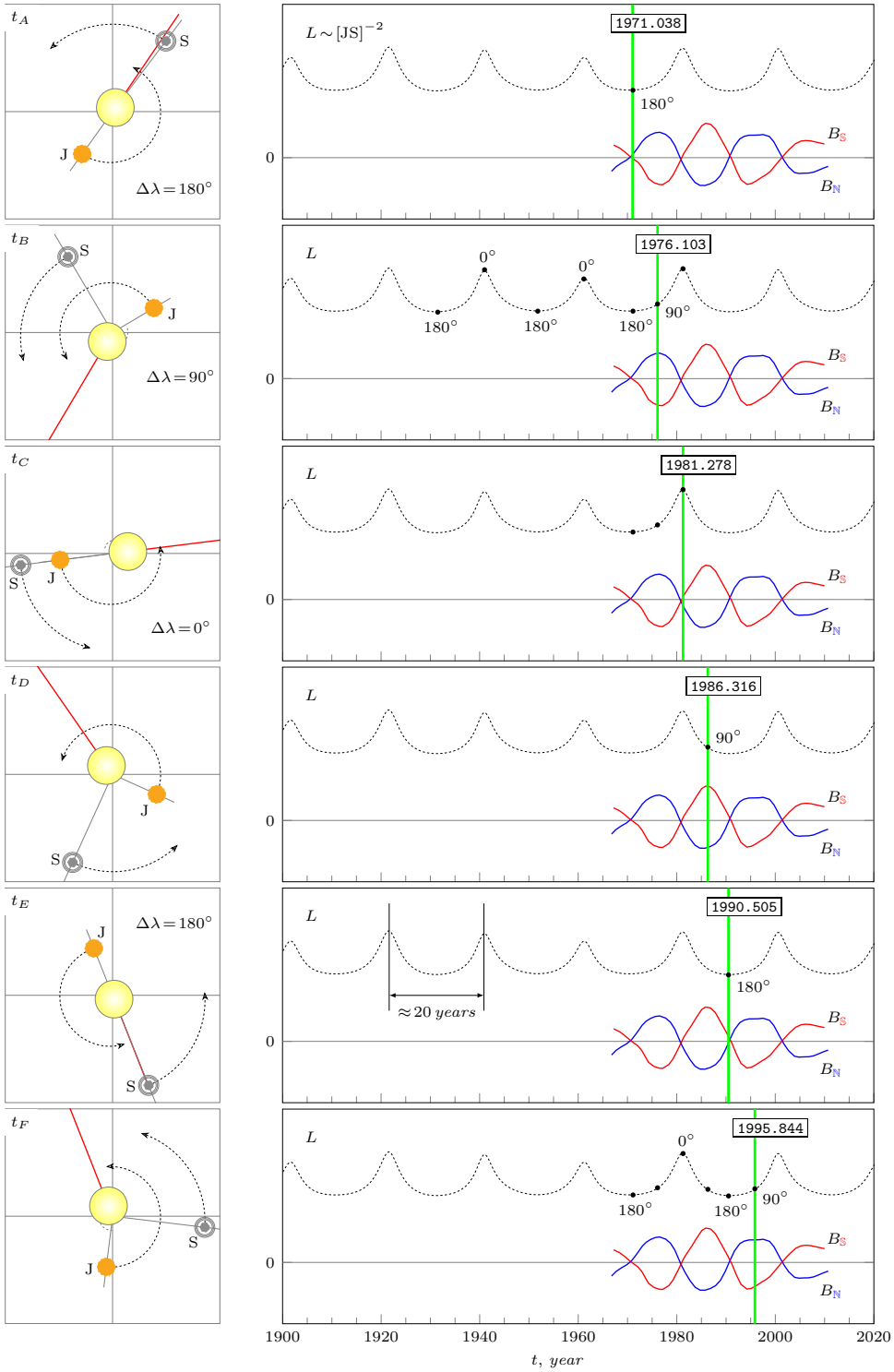

Figure 7. Dependence of the magnetic field strengths at the ℕ and 𝕊 solar poles on the *Jupiter-Saturn* mutual arrangement represented via L and angular distance $\Delta\lambda$. The Sun is represented with the yellow disk; J, S are Jupiter and Saturn, respectively.

of the Sun's magnetosphere is a regular process with the period of about 10 years. This allows assuming that:

> *The Sun's poloidal magnetic field is absent when angular distance $\Delta\lambda$ between the Jupiter and Saturn in the barycentric frame of reference is* 0° *or* 180°*. When* $\Delta\lambda = 90^\circ$*, the poloidal magnetic field at the solar poles reaches its extremum.*

The sufficiency of accounting for the effect of the Jupiter and Saturn on the Sun's magnetosphere poloidal component may be also demonstrated in the following way. Let us calculate parameters of the Sun's orbital motion about the Solar System barycenter based on the *simplified* Solar System model consisting of the Sun, Jupiter and Saturn. In the general case, the Sun's radius-vector $\underline{r}$ and orbital speed vector $\underline{v}$ may be defined in the barycentric frame of reference as follows:

$$\underline{r} = \frac{1}{M_\odot} \sum_{i=1}^{n} \underline{r}_i m_i \ , \quad \underline{v} = \frac{d\underline{r}}{dt} \ , \tag{3}$$

where n is the total number of the considered gravitating bodies of the system except for the Sun; m_i and $\underline{r}_i$ are the mass and radius-vector of the i-th body, respectively; $M_\odot$ is the solar mass.

Let us compare the obtained series of $|\underline{r}|$ and $|\underline{v}|$ values for the simplified Solar System with analogous series for the complete Solar System. These time series are presented pairwise in Fig. 8. One can clearly see that the considered "simplification" of the Solar System has not significantly affected the character of the Sun's orbital speed variation Δv ; this is demonstrated by correlation factor $\mathcal{R}$. Undoubtedly, other giant planets also affect the Sun's orbital speed variability; however, relevant amplitudes are considerably lower, while relevant periods are considerably longer.

To obtain one more justification for sufficiency of considering the "simplified" Solar System model consisting of the Sun, Jupiter and Saturn, let us compare angular momentum (moment of momentum) for different hypothetical variants of the Solar System. Let $\underline{\mathbf{K}}(t)$ be the angular momentum of the complete Solar System:

$$\underline{\mathbf{K}}(t) = \sum_{i=1}^{n} \underline{r}_i \times m_i \underline{v}_i = const \ , \tag{4}$$

where n is the total number of the Solar System objects including the Sun. Formula (4) allows calculation of angular momentum $\underline{\mathbf{K}}$ for different variants

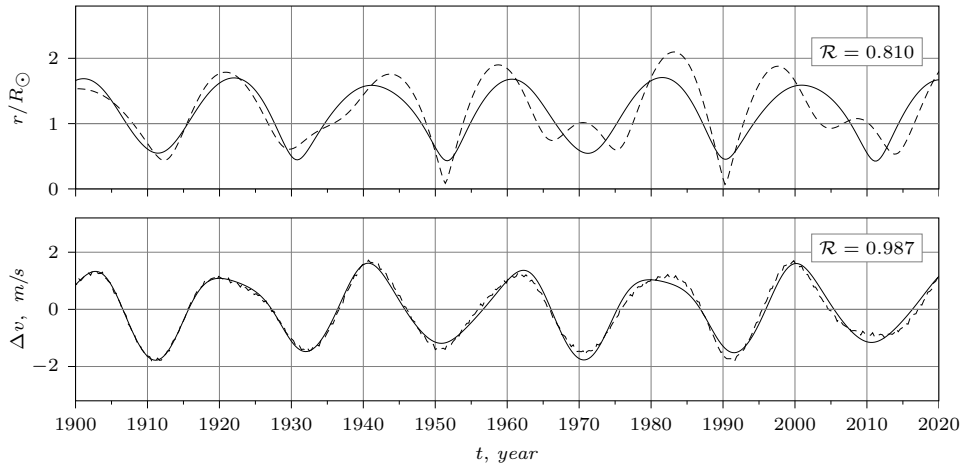

Figure 8. Pairwise comparison of variations in the Sun's orbital radius $r = |\underline{r}|$ and orbital speed Δv for two Solar System configurations: the complete variant(dashed line) and "simplified" variant (solid line) when only the Sun. Jupiter and Saturn are considered. $\mathcal{R}$ is the correlation coefficient.

of the Solar System composition. The calculation showed (see Table 2) that the average angular momentum $\bar{\mathbf{K}}^*$ for the Solar System version we have chosen (Sun, Jupiter and Saturn) is 86.4% of the average $\bar{\mathbf{K}}$ value of the complete Solar System; this also confirms the acceptability of the version under consideration.

Table 2. Ratios between the constant components of angular momentum $\bar{\mathbf{K}}^*$ and $\bar{\mathbf{K}}$ and their mutual correlation coefficients $\mathcal{R}$.

		$\mathcal{R}$	$\bar{\mathbf{K}}^*/\bar{\mathbf{K}}$
	The Solar System	1	1
1.	Sun	0.001	0.1
2.	Sun – Jupiter	0.491	0.615
▷ 3.	Sun – Jupiter – Saturn	0.974	0.864
4.	Sun – Jupiter – Saturn – Uran	0.979	0.918
5.	Sun – Jupiter – Saturn – Uran – Neptun	0.994	0.998

Thus, based on all the above we can affirm that the existence of the poloidal alternating magnetic field of the Sun (Fig. 6) is caused exclusively by the ≈20-year periodicity of the mutual *Jupiter-Saturn* arrangement with respect to the Solar System barycenter.

4 Generation mechanism of the Sun's poloidal alternating magnetic field

Long-term observation over the Sun's magnetic field [11] enabled formation of time series (Fig. 1) representing the dynamics of the poloidal magnetic field strengths $B_{\mathbb{N}}$, $B_{\mathbb{S}}$ at the north and south solar poles.

As shown earlier (Fig. 6), variation in the Sun's orbital speed Δv has the same 20-year period as oscillations of the poloidal alternating magnetic fields at the solar poles. Assume that the Sun's orbital speed variation underlies the mechanism for generation of this magnetic field. Therefore, inside the Sun there should be a certain mechanism based on which the variation in the Sun's orbital speed initiates the generation of the poloidal alternating magnetic field.

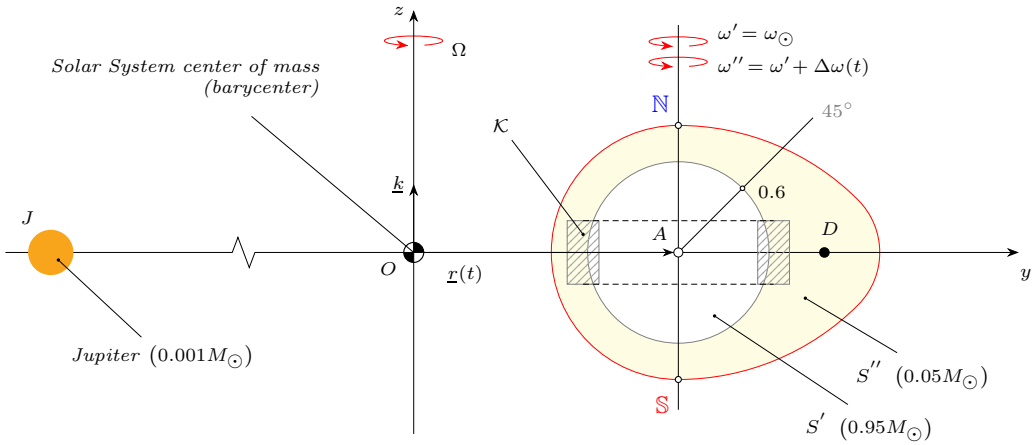

Figure 9. Meridional section of the Sun with plane Oyz. The equatorial centrifugal bulge D is the Sun's region S'' deformed by centrifugal forces as a result of the *Sun-Jupiter* system rotation about the Solar System barycenter with angular velocity Ω.

Let us introduce into consideration fixed Cartesian frame of reference $Oxyz$ (Fig. 9) where origin O is located at the Solar System center of mass, while plane Oxy coincides with the ecliptic.

Assume that the axis of the Sun's own rotation is parallel to axis Oz. Let us assign to axes Ox, Oy, Oz unit orts $\underline{i}$, $\underline{j}$, $\underline{k}$, respectively. The Sun's instantaneous position, i.e., its center of mass A, is defined in the $Oxyz$ system by radius-vector $\underline{r}(t)$.

Paper [14] has shown that, mechanically, the Sun is a deformable body; based on helio-seismological data (Fig. 3), its structure may be represented as two characteristic regions. The first rigid region S' with mass $0.95M_{\odot}$ includes the Sun's core and radiative-transport zone. The other deformable

region S'' is an adjacent spherical layer $0.05M_\odot$ in mass which consists of the convective-transport zone and photosphere. Thus, we will regard the Sun as a non-uniformly orbiting rigid body S' surrounded by deformable region S'' whose mass is approximately 19 times lower than that of region S'.

Angular velocity Ω of the Sun's orbital motion about barycenter O corresponds to the period of about 11.86 years. This period is mainly governed by the *Sun-Jupiter* system rotation about the barycenter in the ecliptic plane Oxy. At the same time, the Sun is affected by centrifugal forces deforming the outer region S'', which manifests itself as formation of the gravitational anomaly [14] or centrifugal bulge. The centrifugal bulge volume and mass depend on the Sun's orbit parameters, and, hence, their values vary with time. To describe this bulge, let us put into consideration point D located in the equatorial plane at some distance from the axis of the Sun's own rotation (Fig. 9).

If we assume that the Sun orbits uniformly (circular motion), centrifugal bulge D in region S'' will be fixed with respect to S'. If, however, the Sun – Jupiter system is supplemented with Saturn, there arises the Sun's orbital speed variation Δv with the period of $\approx$20 years; we believe that this is the main reason for *the emergence* of tangential forced oscillations of region S'' centrifugal bulge D about the Sun's central part.

Define angular velocities for regions S' and S'':

$$\omega' = \omega_\odot \,, \quad \omega'' = \omega' + \Delta\omega(t) \,, \tag{5}$$

where $\Delta\omega$ is the angular velocity of the tangential forced oscillations of the region S'' centrifugal bulge D with respect to S'. Additional angular velocity $\Delta\omega$ stems from the Sun's orbital speed variation Δv. Formula (5) shows that the Sun's own rotation with speed $\omega_\odot$ is excluded from consideration.

There is an opinion that the poloidal alternating magnetic field is generated in *the tachocline*[3]; however, the plasma rotation in these regions does not change its direction and, thus, conditions for the magnetic field inversion are *a priori* excluded. Therefore, we do not consider *the tachocline* as a region where the Sun's poloidal alternating magnetic field is generated.

We believe that the poloidal alternating magnetic field is to be generated in the equatorial region at the $S' - S''$ contact boundary because, to our opinion, only there the solar plasma *reverse rotation* gets fully realized with the about 10-year interval due to oscillations of the region S'' centrifugal bulge D in the Sun's equatorial plane. For this purpose, let us select in

[3]Helio-seismology data show that inside the Sun there is a region where *the tachocline* undergoes a sharp variation in the angular velocity of the solar matter rotation. The concept of tachocline was proposed in 1992 in paper [15].

the Sun's equatorial region at the interaction boundary between rigid Sun's central part S' and deformable spherical layer S'' a torus-like region $\mathcal{K}$ (Fig. 9) with the symmetry axis coinciding with the Sun's own rotation axis.

What occurs in region $\mathcal{K}$? Let us consider the Sun's equatorial section by ecliptic plane Oxy (Fig. 10). Torus-like region $\mathcal{K}$ is marked by hatch-

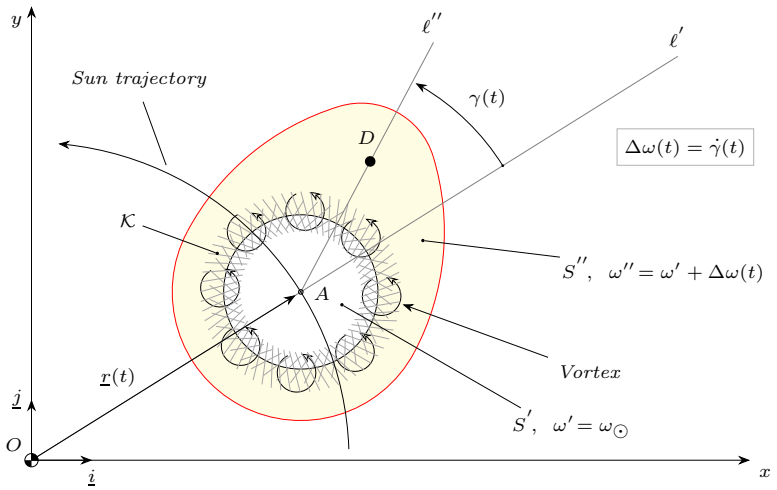

Figure 10. The Sun's equatorial section. Region S'' deformed by centrifugal forces. Line l' that is ray $[OA)$ indicates the direction of the centrifugal force applied to the Sun's center of mass A. Line l'' that is ray $[AD)$ sets the centrifugal bulge D position with respect to direction l'.

ing; this is the region of transition from the Sun's central part S' to outer part S''. Due to forced oscillations of the region $\mathcal{K}$ centrifugal bulge D relative to S'', plasma vortices get formed mechanically (to our opinion) in region S'; rotation planes of the vortices are mainly parallel to the Sun's equatorial plane. The rotation sense of the vortices is defined exclusively by the difference between angular velocities ω' (region S') and ω'' (region S''), namely, by the sign of the relative angular velocity $\dot{\gamma}(t)$. Forced oscillations of the S'' centrifugal bulge with respect to ray l' initiate sequential changes in the rotation sense of *the localized solar plasma vortices* in region $\mathcal{K}$ with the period of about 10 years.

Generation of the alternating magnetic field. We assume that the poloidal alternating magnetic field of the Sun is defined by the sum of magnetic fields of all the vortices emerging in region $\mathcal{K}$. Let us characterize the vortex magnetic field by magnetic field strength vector $\underline{b}$ in the vortex geometric center.

Consider the vortex formation process from the point of view of an Observer looking from the north solar pole. Fig. 11 illustrates the process of generation of vortices during the time interval from t_A to t_C (10 years), just from their initiation till disappearance. For comparing characteristic positions of the region S'' centrifugal bulge D, we have added variations Δv in the Sun's orbital speed and time series representing the poloidal magnetic fields $B_{\mathbb{N}}(t)$, $B_{\mathbb{S}}(t)$ at the respective solar poles.

In our case, analysis of the Sun's orbital speed variation within the chosen time interval from t_A to t_C shows that angular velocity ω'' is lower than angular velocity ω'. This results in formation of vortices rotating clockwise. Since we *a priori* know from observations the direction of magnetic field strength vector $\underline{B}_{\mathbb{N}}$, the following condition should be fulfilled for each clockwise-rotating vortex generating magnetic field b:

$$\underline{b} \uparrow\uparrow \underline{B}_{\mathbb{N}} \,. \tag{6}$$

The plasma vortex comprises current rings consisting of both positive and negative particles. Depending on the moving charge sign[4], let us characterize each current ring by the magnetic field strength vector $\underline{b}^p$ or $\underline{b}^e$ in the central part of the current ring. Thus, the vortex magnetic field b is defined by a combination of magnetic fields of all its current rings, i.e., the total magnetic field vector $\underline{b}$ may be represented for the vortex under consideration as follows:

$$\underline{b} = \sum \underline{b}^p + \sum \underline{b}^e \,, \quad \text{where} \qquad \left|\sum \underline{b}^e\right| > \left|\sum \underline{b}^p\right| \,. \tag{7}$$

Such a relation between the magnetic fields of current rings follows from the Biot – Savart – Laplace law under the condition of elevated electron concentration in the Sun's equatorial region at the interface between the zones of radiative and convective transport. This condition stems from the consistency of the vortex magnetic fields b with the observed direction of the strength vector $\underline{B}_{\mathbb{N}}$. Let us distinguish in Fig. 11 three specific time moments:

t_A: the moment of inversion ($B_{\mathbb{N}} = B_{\mathbb{S}} = 0$).
/*The onset of generation of the subsequent poloidal magnetic field.*/
Angular speed $\dot{\gamma} = 0$.
The Sun's orbital speed $|\underline{v}| = min$;

t_B: the magnetic field strength is maximal, i. e. $|\underline{B}_{\mathbb{N}}| = |\underline{B}_{\mathbb{S}}| = max$.
Angular speed $|\dot{\gamma}| = max$.

[4]Here we can mention the commonly known right-hand rule for determining the magnetic field direction in the case of circular motion of electrons; the fact that the current direction is opposite to the electron motion direction should be taken into account.

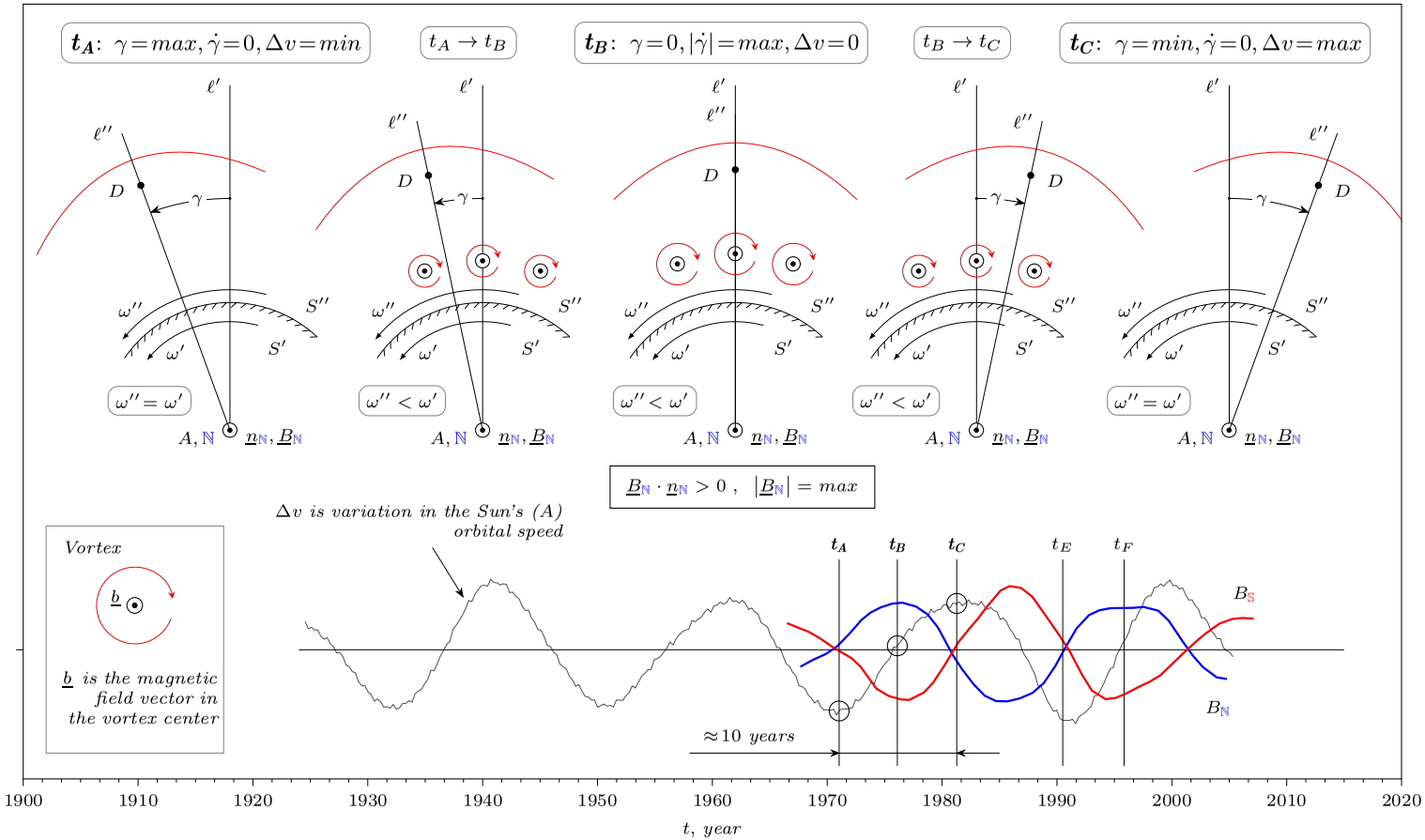

Figure 11. Formation of vortices generating the Sun's poloidal magnetic field in the interface layer $\mathcal{K}$ between the radiation-transport zone $S^{'}$ and convective-transport zone $S^{''}$ due to the difference in their angular speeds ω' and ω'', where $\omega'' = \omega' + \dot{\gamma}$.

$\boldsymbol{t_C}$**:** the moment of inversion ($B_{\mathbb{N}} = B_{\mathbb{S}} = 0$).
/*The onset of generation of the subsequent poloidal magnetic field.*/
Angular speed $\dot{\gamma} = 0$.
The Sun's orbital speed $|\underline{v}| = max$;

Time series presented in Fig. 11 indicate a defining role of the Sun's orbital speed variation Δv about 20 years in period in the formation of the Sun's poloidal alternating magnetic field. Thus, we have established an unambiguous cause-and-effect relationship between different-physical-nature processes participating in generation of the Sun's poloidal magnetic field.

Therefore, a great number of vortices with co-directed magnetic field vectors $\underline{b}$ emerge in region $\mathcal{K}$. Just the combination of those magnetic fields forms the observed Sun's poloidal alternating magnetic field. Inversion of the vortex rotation sense leads to inversion of the Sun's poloidal magnetic field. Fig. 12 presents the structure of the Sun's magnetosphere corresponding to the time moments when the poloidal magnetic field strengths at the solar poles reach their maxima; this event takes place every 20 years.

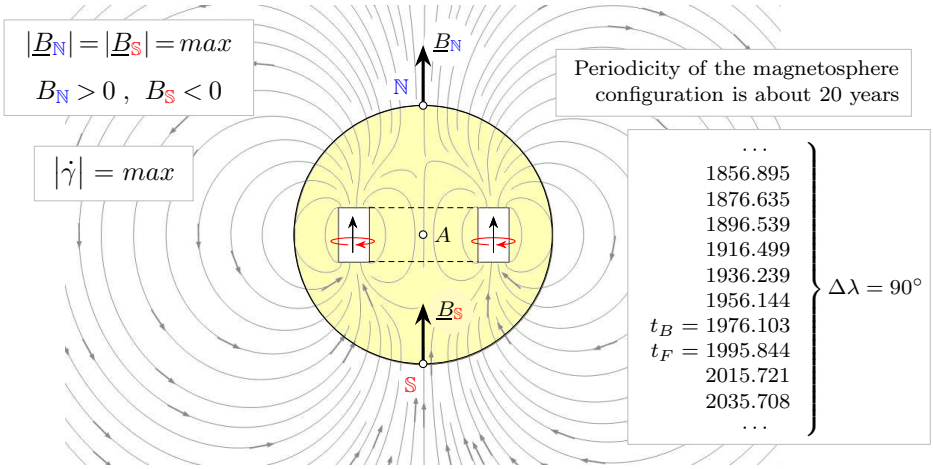

Figure 12. The Sun's poloidal magnetic field at the moment of its maximal intensity; the field has been formed by a group of vortices in region $\mathcal{K}$ at the contact boundary between the radiative and convective transport zones. The figure presents a fragment of sequence of calendar dates corresponding to this state of the magnetic field.

5 Simulation of the reverse motion of the Sun's centrifugal bulge

Using the mathematical pendulum as a model, let us demonstrate the mechanical nature of forced tangential oscillations of the region S'' centrifugal

bulge D with respect to the Sun's central rigid part S'.

Theoretical model. Fig. 13 illustrates the theoretical scheme of the pendulum simulating the forced oscillations of the region S'' centrifugal bulge D with respect to the Sun's central rigid part S' whose center of mass is at point A. The model is based on the concept of a pendulum with the kine-

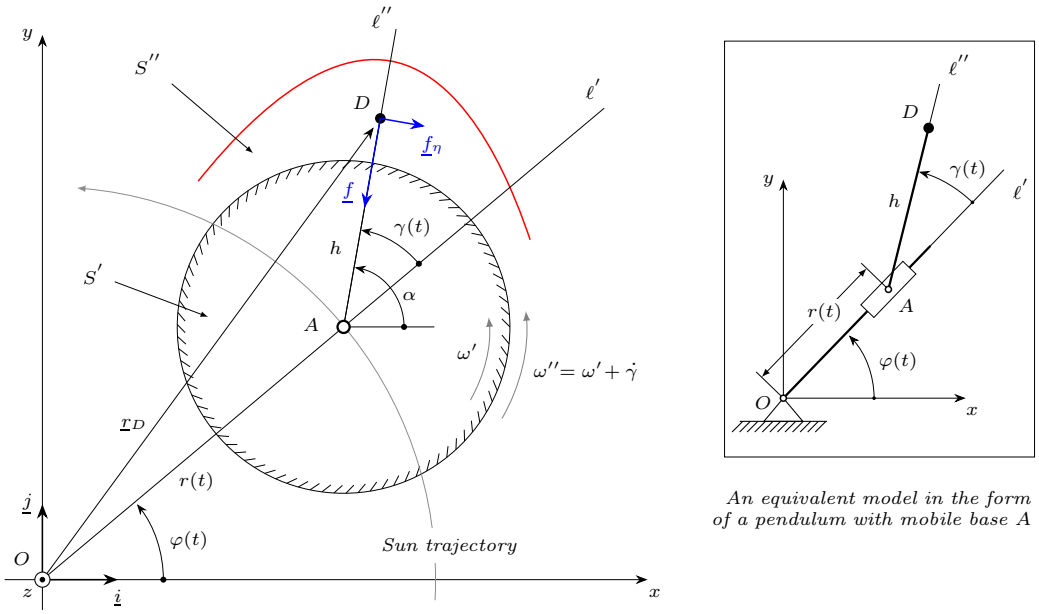

An equivalent model in the form of a pendulum with mobile base A

Figure 13. The pendulum (right panel) simulating oscillations of centrifugal anomaly D in region S''.

matic excitation of base A. The pendulum is a weightless rigid rod AD with length h which is hinged at point A on a mobile weightless element able to move friction-less along a weightless guide (ray l') hinged at fixed point O. Radius-vector $\underline{r}_D$ sets the current position of point D with mass m which undergoes forced oscillations in plane Oxy relative to ray l'. Ray l' points the direction of the resulting centrifugal force applied to point A, which arises due to *the Sun-Jupiter-Saturn* system rotation about barycenter O. Kinematics of the pendulum base (point A) is defined by the Sun's ephemeris, or, more exactly, by radius-vector $\underline{r}(t)$ in the barycentric frame of reference $Oxyz$.

The centrifugal bulge mass m is generally a function of $\underline{r}(t)$. Assume that $m = const$, since our task is to demonstrate the mechanism of relationship between the Sun's orbital speed and tangential oscillations of centrifugal bulge D.

Let us define the point A instantaneous coordinates via $r(t) = |\underline{r}(t)|$ and rotation angle $\varphi(t)$ calculated through $\underline{r}(t)$. The specified kinematics of cen-

tral rigid region $S^{'}$ in plane Oxy leads to relevant tangential oscillations of deformable region $S^{''}$ about $S^{'}$. Deviation of region $S^{''}$ centrifugal bulge D is characterized by angle $\gamma(t)$ which is set off in the direction from ray $l^{'}$ to $l^{''}$. Assume that $\gamma > 0$ in the case of the counterclockwise deviation; otherwise, $\gamma < 0$.

Dynamics equation. The force balance equation for material point D in Fig. 13 will be written as follows:

$$m\,\underline{\ddot{r}}_D = \underline{f} + \underline{f}_\eta\ , \quad \text{where} \qquad \underline{r}_D = x(t)\,\underline{i} + y(t)\,\underline{j} + \cancelto{0}{z(t)}\,\underline{k}\ . \tag{8}$$

Here $x(t), y(t), z(t)$ are the instantaneous coordinates of material point D with mass m in barycentric frame of reference $Oxyz$. Assume that point D is subject to only two forces. These are holding force $\underline{f}$ acting along ray $l^{''}$ towards point A and generalized "viscous" friction force $\underline{f}_\eta$. We take friction force $\underline{f}_\eta$ to mean all that hinders relative motion of the region $S^{''}$ centrifugal bulge D.

Let us present equation (8) in the coordinate form. For convenience, put into consideration auxiliary angle α.

$$\alpha = \varphi + \gamma\ . \tag{9}$$

Then expressions for $\underline{f}$ and $\underline{f}_\eta$ take the following form:

$$\underline{f} = f \begin{pmatrix} -\cos\alpha & 0 \\ 0 & -\sin\alpha \end{pmatrix} \begin{pmatrix} \underline{i} \\ \underline{j} \end{pmatrix} \quad \text{or} \quad \begin{pmatrix} f_x \\ f_y \end{pmatrix} = f \begin{pmatrix} -\cos\alpha \\ -\sin\alpha \end{pmatrix} \tag{10}$$

and

$$\underline{f}_\eta = \eta\, h\dot{\gamma} \begin{pmatrix} \sin\alpha & 0 \\ 0 & -\cos\alpha \end{pmatrix} \begin{pmatrix} \underline{i} \\ \underline{j} \end{pmatrix} \quad \text{or} \quad \begin{pmatrix} f_{\eta_x} \\ f_{\eta_y} \end{pmatrix} = \eta\, h\dot{\gamma} \begin{pmatrix} \sin\alpha \\ -\cos\alpha \end{pmatrix}\ . \tag{11}$$

Here η is the generalized coefficient of solar plasma "viscous" friction in region $\mathcal{K}$ (Figs. 9 and 10).

Then let us write down the radius-vector $\underline{r}_D$ projections on axes Ox, Oy and differentiate them twice with respect to time.

$$\begin{pmatrix} x \\ y \end{pmatrix} = r \begin{pmatrix} \cos\varphi \\ \sin\varphi \end{pmatrix} + h \begin{pmatrix} \cos\alpha \\ \sin\alpha \end{pmatrix}\ , \tag{12}$$

$$\begin{pmatrix} \ddot{x} \\ \ddot{y} \end{pmatrix} = \left(\ddot{r} - r\dot{\varphi}^2\right) \begin{pmatrix} \cos\varphi \\ \sin\varphi \end{pmatrix} + \left(2\dot{r}\dot{\varphi} + r\ddot{\varphi}\right) \begin{pmatrix} -\sin\varphi \\ \cos\varphi \end{pmatrix} + \\ + h\ddot{\alpha} \begin{pmatrix} -\sin\alpha \\ \cos\alpha \end{pmatrix} - h\dot{\alpha}^2 \begin{pmatrix} \cos\alpha \\ \sin\alpha \end{pmatrix}\ . \tag{13}$$

Substitute relations (10), (11) and (13) into force balance equation (8):

$$\left(\ddot{r} - r\dot{\varphi}^2\right)\begin{pmatrix}\cos\varphi\\ \sin\varphi\end{pmatrix} + \left(2\dot{r}\dot{\varphi} + r\ddot{\varphi}\right)\begin{pmatrix}-\sin\varphi\\ \cos\varphi\end{pmatrix} +$$
$$+ h\ddot{\alpha}\begin{pmatrix}-\sin\alpha\\ \cos\alpha\end{pmatrix} - h\dot{\alpha}^2\begin{pmatrix}\cos\alpha\\ \sin\alpha\end{pmatrix} = \frac{f}{m}\begin{pmatrix}-\cos\varphi\\ -\sin\varphi\end{pmatrix} + \frac{\eta}{m}\,h\dot{\gamma}\begin{pmatrix}\sin\alpha\\ -\cos\alpha\end{pmatrix} . \quad (14)$$

Let us simplify the obtained set of equations. For this purpose, multiply the left and right parts of the first equation (projection on axis Ox) by $\boxed{-\sin\alpha}$ and those of the second equation by $\boxed{\cos\alpha}$; sum up the obtained equations. As a result of transformation, obtain a differential equation for determining angle $\gamma(t)$.

$$\boxed{h\ddot{\gamma} = -\frac{\eta}{m}\,h\dot{\gamma} - h\ddot{\varphi} + \left(\ddot{r} - r\dot{\varphi}^2\right)\sin\gamma - \left(2\dot{r}\dot{\varphi} + r\ddot{\varphi}\right)\cos\gamma\,.} \quad (15)$$

This equation does not contain holding force f, which makes simpler solution[5] of the defined task (8), i.e., determination of the angle $\gamma(t)$ variation character for the initially preset trajectory of point A (Sun's center of mass).

For the second-order differential equation (15), let us define the Cauchy problem with the following initial conditions:

$$\boxed{\gamma(t)\Big|_{t=t_0} = \gamma_0\,, \quad \dot{\gamma}(t)\Big|_{t=t_0} = 0\,.} \quad (16)$$

The ray l'' periodical forced deviation (characterizing the position of centrifugal bulge D) by angle γ leftward or rightward with respect to l' is governed by the Sun's orbital speed variation Δv. However, there is a specific fact: the angle γ_0 initial value, as well as settings h and η of the pendulum under consideration, is unknown. Nevertheless, we know that when the deviation angle is maximal ($\gamma = \gamma_0 > 0$), the Sun's orbital speed $|\underline{v}|$ is minimal. Hence, processes $\gamma(t)$ and $\Delta v(t)$ are opposite in phase, while the moments of inversion (when $B_{\mathbb{N}} = B_{\mathbb{S}} = 0$) correspond to moments of their extremums. All the above allows defining a criterion for quantitative estimation of the angle γ_0 selection from the range of $-\pi/2$ to $\pi/2$ and optimal parameters h and η of the considered conditional model (the pendulum with kinematic base excitation).

The problem solution algorithm is as follows. Initial values of the pendulum parameters (e.g. h, η and initial angle γ_0) are to be set for time

[5] If later it becomes necessary to define f, then the same transformation will be performed but with multiplying the first equation by $\cos\alpha$ and the second one by $\sin\alpha$.

moment t_0 when the magnetic field inversion is observed. The obtained solution of the differential equation (15) is to be related to the Sun's orbital speed variation Δv via correlation coefficient $\mathcal{R}$ which, ideally, is to tend to -1 because eventually these processes are opposite in phase. Then the process is to be repeated with new refined values of γ_0, h, η. In our case, the iterative process of solving the problem was terminated when there were achieved stable centrifugal bulge oscillations about 20 years in period. Actually, the problem got reduced to searching for the global extremum with respect to several parameters [16, 17].

Simulation results. The model considered showed the possibility of describing the process of emergence of forced oscillations of the region S'' centrifugal bulge D about the Sun's central part as a consequence of the Sun's orbital speed variation Δv. The character of the obtained equation (15) solu-

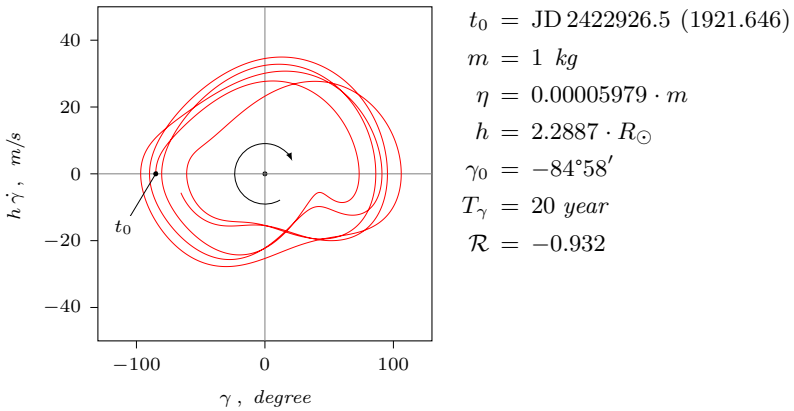

Figure 14. Phase trajectory of the region S'' centrifugal bulge D as a result of solving equation (15) with intial conditions (16).

tion under initial conditions (16) is represented in Fig. 14 by the phase-plane trajectory. In the time interval under consideration, the phase trajectory demonstrates stable character of the centrifugal bulge D oscillations.

Fig. 15 presents the numerical solution of equation (15) in the form of time series $\gamma(t)$ which is compared with the Sun's orbital speed variation Δv and oscillations of the magnetic field strengths $B_{\mathbb{N}}$ and $B_{\mathbb{S}}$ at the solar poles.

Notice that these time series are absolutely consistent with each other. Table 3 lists the values of the *Jupiter-to-Saturn* angular distance $\Delta\lambda$ in the barycentric frame of reference, deviation of the Sun's orbital speed variation from mean $\bar{v}$, and centrifugal bulge D deviation angle γ determined for key moments $t_A, t_B, t_C, \ldots$.

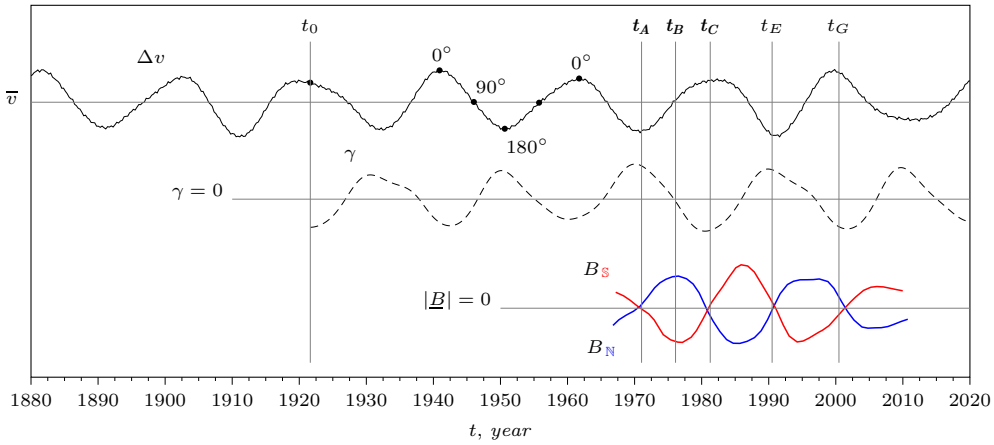

Figure 15. Comparison of the Sun's orbital speed variation Δv, deviation angle γ of centrifugal bulge D, and poloidal magnetic field strengths $B_{\mathbb{N}}$, $B_{\mathbb{S}}$ at the solar poles.

Table 3. Calendar dates of occurrence of specific points of the Sun's poloidal alternating magnetic field and its concominant characteristics: $\Delta\lambda$ is the angular distance between the Jupiter and Saturn; Δv is the Sun's orbital speed variation; γ is the deviation angle of centrifugal bulge D.

	BD	$B_{\mathbb{N}}, B_{\mathbb{S}}$	$\Delta\lambda$, *degree*		Δv, *m/s*	γ, *degree*
t_A	1971.038	0	178.8	(180)	-3.5	99.8
t_B	1976.103	$B_{\mathbb{N}}{}^{+}, B_{\mathbb{S}}{}^{-}$	89.9	(90)	0.8	-6.5
t_C	1981.278	0	1.1	(0)	2.0	-94.3
t_D	1986.315	$B_{\mathbb{N}}{}^{-}, B_{\mathbb{S}}{}^{+}$	90.1	(90)	0.4	13.8
t_E	1990.505	0	179.6	(180)	-2.8	89.0
t_F	1995.844	$B_{\mathbb{N}}{}^{+}, B_{\mathbb{S}}{}^{-}$	90.2	(90)	-0.1	22.9
t_G	2000.471	0	1.2	(0)	3.2	-83.3
t_H	2006.165	$B_{\mathbb{N}}{}^{-}, B_{\mathbb{S}}{}^{+}$	90.1	(90)	-0.5	4.1

The obtained results clearly show that the existence of the poloidal alternating component of the Sun's magnetosphere is fully governed by the Sun's orbital speed variation Δv which is just that initiates relevant forced tangential oscillations of the region S'' centrifugal bulge D with respect to the Sun's central rigid part S'.

6 Sequence of Wolf numbers

In 1843, S.H. Schwabe revealed the presence of the 10-year period while analyzing a time series representing variations in sunspot number during a long time interval [18]. I.e., local maxima alternate with the period of

about 10 years. Then, in 1848, J.R. Wolf proposed a method for quantitative estimation of the solar activity based on the number of spots observed on the solar surface; the method was expressed as

$$W = k\,(10g + s)\,, \tag{17}$$

where W is the measure of solar activity, s is the number of sunspots, g is the number of groups of the observed sunspots, k is the dimensionless coefficient used to bring into consistency the time series formed from Wolf numbers based on direct solar disk observations. One of the first researchers who tried to make apparent the effect of the external factor, namely, the Sun's motion relative to the Solar System barycenter, upon the sunspot formation, was *Paul D. Jose* [19].

Fig. 16 demonstrates the relationship between the Jupiter – Saturn mutual configuration L and observed oscillations in the poloidal magnetic field strengths $B_{\mathbb{N}}$, $B_{\mathbb{S}}$ at the solar poles via *forced oscillations* of centrifugal bulge D characterized by angle $\gamma(t)$. In the lower part of the same figure

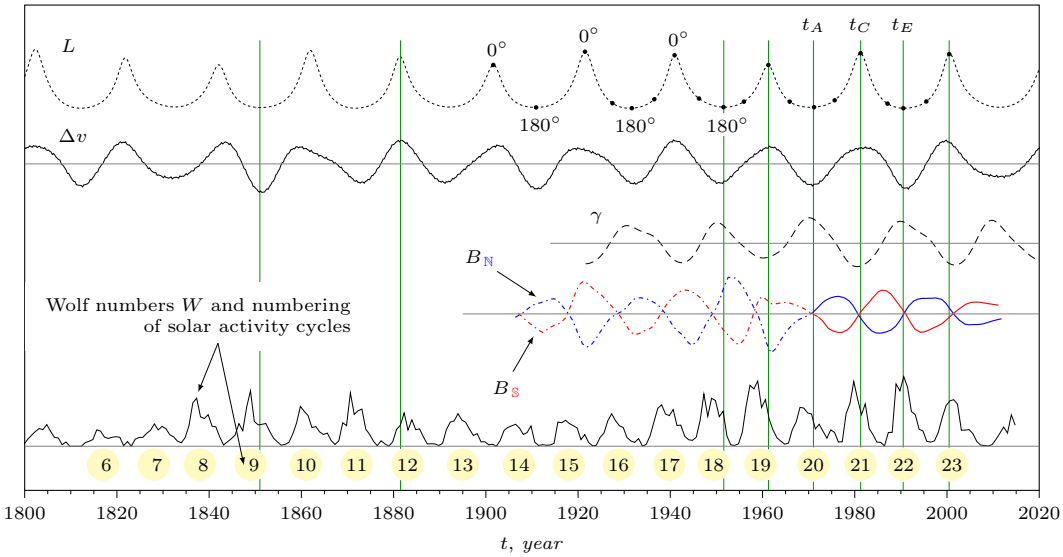

Figure 16. The sequence of processes governing formation of the Sun's alternating poloidal magnetic field. L demonstrates the Jupiter – Saturn spatial configuration; Δv is the Sun's orbital speed variation; $B_{\mathbb{N}}$, $B_{\mathbb{S}}$ are the strengths of the poloidal magnetic field at the solar poles; t_A, t_C, t_E are the moments of inversion.

there is presented a sequence of Wolf numbers W constructed based on the SILSO data [20], where a conditional serial number of 6 to 23 is assigned to each W maximum.

As shown above, the existence of the Sun's poloidal alternating magnetic field is governed by an external determining factor, i.e., repetition of

the Jupiter – Saturn mutual arrangement in the barycentric frame of reference with the period of about 20 years. This factor affects the Sun's orbital speed, which manifests itself as the speed variation Δv with the period of about 20 years. One can clearly see that, within the time interval from 1970s till now, Wolf number minima are always observed between two subsequent inversions of poloidal magnetic field B; such a minimum is sometimes accompanied by a maximum, but never by another minimum. Since the nature of the Sun's poloidal alternating magnetic field is defined exclusively by the Jupiter and Saturn dynamics, time series L constructed based on their ephemerides becomes an event-and-time scale (Fig. 17) that allows unambiguously indicating dates of past and future inversions of the Sun's magnetic field as well as time limits within which number W will be minimal. Accuracy of predicting calendar dates of the Sun's poloidal magnetic field inversions depends on the accuracy of the Jupiter and Saturn ephemerides.

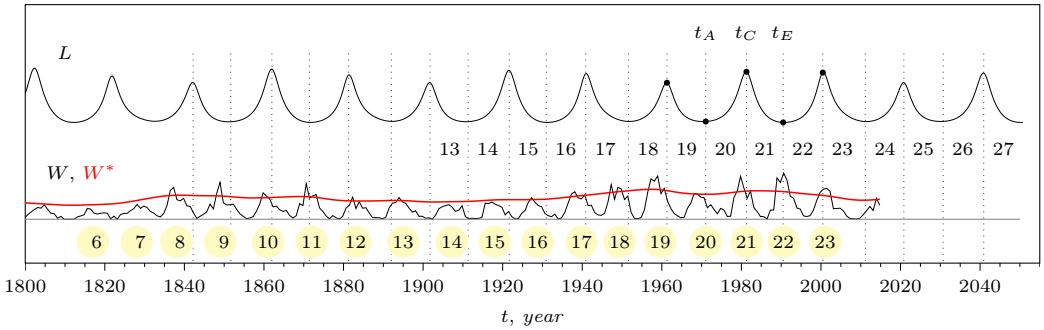

Figure 17. L is the parameter characterizing the distance between the Jupiter and Saturn; W, W^* are the Wolf numbers. W^* (red line) reflects the assessment level of *the natural solar activity* via Wolf numbers in the hypothetical absence of the Sun's alternating poloidal magnetic field.

Based on the above, it is possible to affirm that cyclicity of the sequence of Wolf numbers W is governed by the "half-period" of oscillations in the Sun's magnetosphere poloidal component which, in its turn, is induced by the 20-year-period repetition of the Jupiter – Saturn mutual configuration. Let us introduce a concept of *natural solar activity*, that is, a certain stochastic process of the solar-surface spot formation in the absence of the poloidal component of the Sun's magnetosphere. The observed maxima in the sequence of Wolf numbers W reflect, to some extent, the level of *natural solar activity* W^* (Fig. 17).

In other words, we observe the effect of a deterministic process in the form of poloidal alternating magnetic field B on the stochastic process of spot formation on the solar surface, the result of which is the commonly known sequence of Wolf numbers W. Thus, observation over the dynamics

of emergence and disappearance of sunspots is, in essence, indirect observation over the Sun's magnetosphere poloidal component. Each solar activity minimum W always falls on the interval between two subsequent inversions of poloidal magnetic field B, contrary to the solar activity maximum that can be located both to the left and right of the moment of inversion. This is just why the cycles of solar activity W should be counted not by maxima as is customary at present, but by minima; given the moment of a minimum is *always* between the neighboring inversions, it is reasonable to relate numbering of the solar activity cycles to serial numbers of time intervals between the moments of the poloidal magnetic field inversion or, metrologically more valid, to the moments of the time series $L(t)$ extremums (Fig. 17).

7 Conclusions

The research results presented in this paper were obtained mainly by using the heuristic approach in searching for and constructing a sequence of the cause-and-effect relationships that in total give the answer to the raised issue. This sequence of processes is given in Fig. 16. Diagram (18) demonstrates a unidirectional relationship between the Jupiter – Saturn mutual configuration $L(t)$ and Sun's orbital speed variation Δv which, in its turn, initiates forced oscillations of the Sun's centrifugal bulge which are expressed via angle γ and result in generation of the Sun's poloidal alternating magnetic field in the toroidal region $\mathcal{K}$.

$$\overbrace{L}^{\textit{Jupiter–Saturn}} \longrightarrow \overbrace{\Delta v \longrightarrow \gamma \longrightarrow \begin{matrix} B_{\mathbb{N}}{}^{\pm} \\ B_{\mathbb{S}}{}^{\mp} \end{matrix} \longrightarrow W}^{\textit{Sun}} \tag{18}$$

7.1 Poloidal magnetic field of the Sun

> The nature of the Sun's poloidal alternating magnetic field is caused exclusively by the periodicity of the Jupiter – Saturn spatial configuration in the barycentric frame of reference.

The Sun and Jupiter rotate about the Solar System barycenter with the period of about 11.86 years. Putting into consideration the Saturn with its period of 29.45 years in the process of calculating the Sun's ephemeris

results in appearance of the Sun's orbital speed variation Δv about 20 years in period. This initiates formation inside the Sun of the toroidal region $\mathcal{K}$ where there arise conditions necessary for generation of the poloidal alternating magnetic field about 20 years in period.

7.2 The role of the Sun's own rotation

> The Sun's own rotation does not affect the mechanism for generation of the Sun's poloidal alternating magnetic field but only makes a static correction to the centrifugal bulge deviation angle.

7.3 Event-and-time scale

> Time series $L(t)$ is an event-and-time scale allowing synchronization of occasional and inconsistent data related to the appearance of Sun-Earth relationships.

Time moments when the Jupiter and Saturn are in line with the Sun either on its one side ($\lambda = 0°$) or on opposite sides ($\lambda = 180°$) correspond to the moments of the Sun's poloidal field inversion. Thus, knowing the Jupiter's and Saturn's ephemerides in the barycentric frame of reference, we can calculate time moments at which the Sun's field inversion either occurred in the past or is expected in future.

Process $L(t)$ makes possible metrologically correct synchronization of the fragments of inconsistent observations over the magnetic field strength and sunspots (Wolf numbers W). As shown earlier, time moments of the $L(t)$ local extremums mandatory correspond to the moments of the Sun's poloidal magnetic field inversion and extremums of the Sun's orbital speed variation Δv. For instance, the dashed line in Fig. 16 represents archival data from fragmentary observations over the Sun's poloidal magnetosphere component, which were systematized by the authors of [5] based on the Wolf number series. We propose that inconsistency between the moments of magnetic field inversion and moments of extremums of the Sun's orbital speed variation, which is shown in Fig. 16, be corrected with taking into account process $L(t)$.

7.4 Natural solar activity

> The observed cyclicity of Wolf numbers W stems from the deterministic effect of the Sun's poloidal alternating magnetic field upon the natural solar activity W^* that is a certain stochastic process manifesting itself as sunspot formation on the solar disk.

This conclusion was made based on comparing (Fig. 16) variations in magnetic field strengths $B_{\mathbb{N}}$, $B_{\mathbb{S}}$ with the sequences of Wolf numbers W. The poloidal alternating magnetic field exerts a certain structuring influence on the plasma behavior in the upper layers of the Sun's convective zone and photosphere. When the magnetic field reaches its maximum, the sunspot number is minimal or they are even fully absent. In fact, the Sun's poloidal magnetic field "manages" the process of sunspots *disappearance*. It may be said that at the moments of inversion (pole flip) in the absence of the poloidal magnetic field there appears the *natural solar activity* characterized by the instantaneous value of W, i.e. $W \approx W^*$. Hypothetically, if it were no 20-year Sun's orbital speed variation, we could observe natural solar activity (the red line in Fig. 17).

References

[1] *Zeeman, Dr. P.* Vii. doublets and triplets in the spectrum produced by external magnetic forces / Dr. P. Zeeman // *The London, Edinburgh, and Dublin Philosophical Magazine and Journal of Science*. "— 1897. "— Vol. 44, no. 266. "— Pp. 55–60. "— https://doi.org/10.1080/14786449708621028.

[2] *Babcock, Horace W.* Mapping the Magnetic Fields of the Sun / Horace W. Babcock, H. D. Babcock // *Astronomical Society of the Pacific*. "— 1952. "— Dec.. "— Vol. 64, no. 381. "— P. 282.

[3] *Babcock, Horace W.* The Sun's Magnetic Field, 1952-1954. / Horace W. Babcock, Harold D. Babcock // *Astrophysical Journal*. "— 1955. "— Mar.. "— Vol. 121. "— P. 349.

[4] *Babcock, Harold D.* The Sun's Polar Magnetic Field. / Harold D. Babcock // *Astrophysical Journal*. "— 1959. "— Sep.. "— Vol. 130. "— P. 364.

[5] *Andrés Muñoz-Jaramillo and Neil R. Sheeley and Jie Zhang and Edward E. DeLuca*. CALIBRATING 100 YEARS OF POLAR FACULAE MEASUREMENTS: IMPLICATIONS FOR THE EVOLUTION OF THE HELIOSPHERIC MAGNETIC FIELD / Andrés Muñoz-Jaramillo and Neil R. Sheeley and Jie Zhang and Edward E. DeLuca // *The Astrophysical Journal*. "— 2012. "— Jun.. "— Vol. 753, no. 2. "— P. 146. "— https://dx.doi.org/10.1088/0004-637X/753/2/146.

[6] *Deubner, Franz-Ludwig*. Helioseismology: Oscillations as a Diagnostic of the Solar Interior / Franz-Ludwig Deubner, Douglas Gough // *Annual Review of Astronomy and Astrophysics*. "— 1984. "— Jan.. "— Vol. 22. "— Pp. 593–619.

[7] *Corbard, Thierry*. Helioseismology from SODISM and HMI Intensity Images / Thierry Corbard, David Salabert, Patrick Boumier // *ArXiv e-prints*. "— 2013.

[8] *Kulikovsky, P. G.* Handbook for amateur astronomer / P. G. Kulikovsky. "— Gos. Izdat. Tekh.-Teor. Liter, 1953.

[9] *Hughes, D. W.* The Solar Tachocline / D. W. Hughes, R. Rosner, N. O. Weiss. "— Cambridge University Press, 2012. "— https://books.google.ru/books?id=-8eZuAAACAAJ.

[10] *NASA JPL Horizons*. "— https://ssd.jpl.nasa.gov/horizons.

[11] *Wilcox Solar Observatory Polar Field Observations*. "— https://wso.stanford.edu/Polar.html.

[12] *Kiryan, Dmitry G.* Modeling the Evolution of a gravitating bodies cluster based on absolutely inelastic collisions / Dmitry G. Kiryan, George V. Kiryan // *ArXiv e-prints*. "— 2021.

[13] *Kiryan, Dmitry G.* Modeling the Evolution of a cluster of gravitating bodies taking into account their absolutely inelastic collisions / Dmitry G. Kiryan, George V. Kiryan // *PAMM*. "— 2021. "— Dec.. "— Vol. 21, no. 1. "— https://onlinelibrary.wiley.com/doi/abs/10.1002/pamm.202100049.

[14] *Kiryan, Dmitry G.* On the effect of the central body small deformations on its satellite trajectory in the problem of the two-body gravitational interaction / Dmitry G. Kiryan, George V. Kiryan // *arXiv:2008.02802*. "— 2020. "— Aug..

[15] *Spiegel, E. A.* The solar tachocline. / E. A. Spiegel, J. P. Zahn // *Astronomy and Astrophysics*. "— 1992. "— Nov.. "— Vol. 265. "— Pp. 106–114. "— https://ui.adsabs.harvard.edu/abs/1992A&A...265..106S.

[16] *Kiryan, D. G.* Resonance Method of the Spectral Analysis RMSA / D. G. Kiryan // The III International Congress on Industrial and Applied Mathematics, ICIAM. "— 1995.

[17] *Kiryan, D. G.* The resonance Method in studying time series / D. G. Kiryan, G. V. Kiryan // Mechanics and control processes. "— SPbPU, 1997. "— Vol. 467. "— Pp. 69–78. "— UDK52+55.

[18] *Schwabe, Heinrich*. Sonnenbeobachtungen im Jahre 1843. Von Herrn Hofrath Schwabe in Dessau / Heinrich Schwabe // *Astronomische Nachrichten*. "— 1844. "— Feb.. "— Vol. 21, no. 15. "— P. 233.

[19] *Jose, Paul D.* Sun's motion and sunspots / Paul D. Jose // *Astronomical Journal, Vol. 70, p. 193*. "— 1965. "— Apr.. "— Vol. 70. "— P. 193.

[20] *SILSO World Data Center*. The International Sunspot Number. "— http://www.sidc.be/silso.